

PROTECTIVE EFFECTS OF A RODGERNSIA SAMBUCIFOLIA FLAVONOID–SCUTELLARIA POLYSACCHARIDE COMPOUND AGAINST PSEUDORABIES VIRUS-INDUCED TESTICULAR INJURY VIA MODULATION OF THE FOXO SIGNALING PATHWAY

J. Li[†], Y. Zhang[†], J. Lin, J. Wei, C. Song and X. Shu^{*}

College of Veterinary Medicine of Yunnan Agricultural University, Kunming 650201, Yunnan Province, China.

[†] These authors contributed equally to this article.

^{*} Corresponding author's E-mail: ynnndsxh@ynau.edu.cn

ABSTRACT

Pseudorabies virus (PRV) is known to induce severe reproductive disorders, yet the molecular mechanisms underlying testicular damage remain unclear. This research aims to explore the impact of PRV infection on porcine testicular (ST) cells and murine testicular tissue, with a focus on the involvement of the FOXO signaling pathway. This study also evaluated the antagonistic effect of compound RS on PRV infection through regulation of this pathway. Analyze differentially expressed genes and enriched pathways in ST cells infected with PRV through transcriptome sequencing. ST cells were infected with PRV and subsequently treated with either the FOXO pathway inhibitor AS1842856 or varying concentrations of RS (12.5, 25, and 50 µg/mL) to evaluate their effects on viral replication and FOXO gene expression. Cell viability was detected by CCK-8, viral load and mRNA expression of FOXO were detected by qPCR. Establish a PRV infected mouse model, observe pathological changes in testicular tissue through HE staining, detect testicular virus concentration, sperm count, and FOXO gene expression. PRV infection caused significant cytopathic effects in ST cells, with transcriptome sequencing identifying 1,650 significantly upregulated genes and 1,359 significantly downregulated genes ($|\log_2FC| \geq 1$, $P < 0.01$). KEGG pathway analysis indicated significant enrichment of these genes in the FOXO signaling pathway, among others. Inhibition of the FOXO pathway markedly reduced viral replication in ST cells. PRV infection upregulated FOXO1 and FOXO4 mRNA expression, while downregulating FOXO3; these alterations were reversed upon RS treatment. In vivo experiments, RS treatment alleviated the pathological damage of mouse testicular tissue caused by PRV, reduced virus concentration in the testes, and partially restored sperm count. Compound RS effectively suppresses PRV replication both in vitro and in vivo by modulating the FOXO pathway and alleviates testicular injury caused by PRV. These findings provide a theoretical basis and identify a promising candidate for developing novel therapeutics targeting PRV-associated reproductive toxicity.

Keywords: *Rodgersia sambucifolia* hemsl flavon; *Scutellaria polysaccharide*; Pseudorabies virus; FOXO signaling pathway

This article is an open access article distributed under the terms and conditions of the Creative Commons Attribution (CC BY) license (<https://creativecommons.org/licenses/by/4.0>)

<https://doi.org/10.36899/JAPS.2026.4.0099>

Published first online May 13, 2026

INTRODUCTION

Pseudorabies virus (PRV) is transmissible among pigs through oral, nasal, transplanted, and intravenous routes, with clinical manifestations varying significantly depending on the age of the infected host (An *et al.*, 2013). Infection typically leads to more severe outcomes in piglets than in adult pigs and sows, often resulting in higher mortality rates (Zheng *et al.*, 2022). PRV infection in boars results in decreased semen quality, testicular swelling, or atrophy, leading to loss of breeding capacity.

Rodgersia sambucifolia hemsl flavons are flavonoids extracted from *Rodgersia sambucifolia* hemsl. Flavonoids generally have antioxidant, anti-inflammatory, antibacterial and other effects. There was studies showing that *Rodgersia sambucifolia* hemsl flavon can inhibit PRV infection of ST cells (Pan *et al.*, 2022). *Scutellaria baicalensis* is a traditional authentic Chinese medicinal herb with a clinical history of over 2000 years (Zhao *et al.*, 2019). Polysaccharides have physiological activities such as hypoglycemic, hypolipidemic, antitumor, antioxidant, immunity enhancement and anti-aging. The RS complex was non-toxic, with no acute or genetic toxicity observed in experimental animals at doses up to 2500 mg/kg body weight (BW) (Pan *et al.*, 2022). RS has been proven in the pre-laboratory test that this traditional Chinese medicine complex can increase the daily weight gain of piglets and enhance the transformation of piglets' lymphocytes and anti-pseudorabies virus infection ability (Shu *et al.*, 2024).

FOXO proteins constitute a subfamily of forkhead box transcription factors, all of which share a highly conserved forkhead domain (Jacobs *et al.*, 2003). In humans, the FOXO family includes four members: FOXO1, FOXO3a, FOXO4, and FOXO6. Structurally, FOXO proteins contain four conserved domains. Among them, FOXO1, FOXO3, and FOXO4 are widely expressed across nearly all tissues, whereas FOXO6 expression is primarily confined to the central nervous system. Unlike other FOXO members, the subcellular localization of FOXO6 is not regulated by PI3K/AKT signaling (Zhou *et al.*, 2019). It has now been found that inhibition of FOXO1 expression has the effect of significantly inhibiting spermatogenic cell apoptosis and improving spermatogenic function in testis-disordered rats (Tran *et al.*, 2021). Continuous expression of FOXO1 in male mice causes marked testicular shrinkage, significant sperm count reduction, and loss of support for spermatogenic cells. Furthermore, FOXO1 plays a critical role in the maintenance of support cell lineage (Goertz *et al.*, 2011). It suggests that the FOXO signaling pathway is associated with the spermatogenic function in male animals.

MATERIALS AND METHODS

Experimental materials: ST cells were provided in lyophilized form by the laboratory. The PRV was provided by the Key Laboratory of Provincial Universities. A total of fifty 7-week-old specific pathogen-free (SPF) male Kunming mice, weighing 20–25 g, were sourced from Kunming Medical University. All animal experiments were approved by the Institutional Animal Care and Use Committee (IACUC) of Kunming Medical University (Approval No. SCXK(Dian)K 2015-0002).

Main instruments and reagents: Rotary evaporator (Xiande--3000, Shanghai Xiande Experimental Instrument Co., Ltd.), freeze dryer (SCIENTZ-18N, Ningbo Xinzhi Biotechnology Co., Ltd.), inverted microscope (XDS-1B, Chongqing Photoelectric Instrument Co., Ltd.), frozen high-speed centrifuge (DHG-9240A, Germany eppend Co., Ltd.), fluorescence quantitative PCR instrument (CFX-96, bio RAD), Australian fetal bovine serum (GIBCO, 2305262rp), DMEM medium (8121677, GIBCO), DNA/RNA Extraction Kit (RC311, TaKaRa), FOXO inhibitor (AS1842856, MCE).

Preparation of RS: Powdered *Rodgersia sambucifolia* Hemsl. was homogenized with 60% ethanol at a solid-to-liquid ratio of 1:60. The mixture was soaked for 24 h, sonicated for 25 min, incubated in a 70 °C water bath for 3 h, and vacuum-filtered. The resulting filtrate was concentrated by rotary evaporation and lyophilized to obtain a dried powder referred to as the *R. sambucifolia* flavonoid fraction. For the extraction of *Scutellaria baicalensis* polysaccharides, plant powder was refluxed with distilled water (1:50, w/v) for 20 min and subsequently sonicated for 15 min. The extract was filtered through filter paper, mixed with 95% ethanol (1:2, v/v), and stored at 4 °C for 24 h. After centrifugation (3,000 × g, 10 min), the resulting precipitate was resuspended and sonicated for another 15 min. The final lyophilized material was confirmed as *S. baicalensis* polysaccharides by FT-IR analysis. The RS complex was prepared by combining *R. sambucifolia* flavonoid fraction and *S. baicalensis* polysaccharides in a 1:1 mass ratio. The complex was then subjected to plant-wide untargeted sequencing, and its chemical composition was characterized using liquid chromatography–tandem mass spectrometry (LC-MS/MS).

Cellular experimental : Cell viability was assessed using CCK-8, while viral load and FOXO mRNA expression were measured by qPCR. 5×10^4 ST cells were inoculated per well in 96-well plates. When the cells grew up to the full monolayer, they were washed with PBS for 1 time, and the drug solution diluted with the maintenance solution was added at the concentrations of 0, 0.98, 1.95, 3.91, 7.81, 15.63, 31.25, 62.50, 125.00, 250.00, and 500.00 µg/mL, and 8 replicate wells were cultured for 48 h. After 48 h of incubation, according to the instructions of the CCK-8 reagent kit, the OD was determined at 450.

Animal experimental : Fifty Kunming mice were randomly divided into Control, PRV, and RS high (1 g/kg) (RS-H), medium (500 mg/kg) (RS-M), and low (250 mg/kg) (RS-L) dosage groups and were gavaged continuously for 7 d. On the 8th d, in addition to the blank control group, the remaining mice were infected by drip-nose infection with TCID₅₀ as $10^{-7.42}$ /0.1 mL of a 20 µL of PRV suspension and 20 µL of saline in the blank control group, and then the mice continued to be gavaged for 3 d. The mice were executed on the 10th d, and the testes were collected.

Pathologic tissue section preparation: The testes were fixed with formaldehyde, rinsed with running water for 10 min, and then dehydrated with alcohol and transparent with xylene. Then they were dipped in wax, embedded, and the wax was trimmed after the wax block was cold cut and solidified. The slices were placed in a constant temperature water tank for spreading. The slices were baked in a thermostatic oven at 58 °C for 8 h. After the slices cooled down, they were stained with H&E staining, and then the slices were taken out to dry at room temperature and sealed with neutral gum.

Sperm count test:The epididymis was taken and placed in a petri dish, and semen was collected by rinsing the epididymal body with 1 mL of saline from a 37 °C water bath. The epididymal rinse fluid was collected along with the epididymis into a 1.5 mL centrifuge tube and sperm were counted using a cell counting plate.

Transcriptome sequencing and data analysis:Total RNA was extracted from ST cells (Control and PRV-infected groups, n = 3 per group) using TRIzol reagent. RNA-seq libraries were constructed and sequenced on an Illumina platform. Differential expression analysis was performed using DESeq2 software. Genes with an absolute fold change ≥ 2 ($|\log_2FC| \geq 1$) and a false discovery rate (FDR)-adjusted P value < 0.01 were considered significantly differentially expressed genes (DEGs). KEGG pathway enrichment analysis was performed using ClusterProfiler software, with $P < 0.05$ indicating statistically significant enrichment.

DNA/RNA extraction and real-time fluorescence quantitative PCR assay:Animal tissues were milled using liquid nitrogen and DNA/RNA extraction kit instructions to extract DNA/RNA. Real-time fluorescence quantitative PCR was performed on DNA/RNA and the primer sequences are shown in Table 1.

Table 1. Preparation of relevant reagents

genus (taxonomy)	Primer name	primer sequence
mice	FOXO1	F: GGGTCCCACAGCAACGATG
		R: CACCAGGGAATGCACGTCC
	FOXO3	F: CTGGGGGAACCTGTCTATG
		R: TCATTCTGAACGCGCATGAAG
	FOXO4	F: GGGCTCAATCTCGCATCTCC
		R: AGACCCATCTATTGGGCCAAA
	β -actin	F: GTGACGTTGACATCCGTAAGA
		R: GCCGGACTCATCGTACTCC
pig	FOXO1	F: CTGAGCAGGATGACCTTGGAGAC
		R: ATGATGGTGCCTGGTGAAGACTG
	FOXO3	F: AGCCACCTTCTCTCCAT
		R: AGCAAGTTCTGATTGACCAA
	FOXO4	F: CAGCACCGCCTCCAGTCATG
		R: TCCAGTCCTTCGCCTCCATCC
	β -actin	F: AACTACCTTCAACTCCATCA
		R:GTACTCCTGCTTGCTGA

Statistical methods :Data from at least three independent experiments are expressed as mean \pm standard deviation. Statistical analyses were performed using one-way ANOVA followed by Tukey's HSD test in GraphPad Prism 10.0. Data are presented as mean \pm SD from at least three independent experiments. Significance: * $P < 0.05$, ** $P < 0.01$ (ns: not significant).

RESULTS

Analysis of the Composition of RS Complex :By conducting plant wide target sequencing on the complex and comparing the LC-MS/MS analysis data with a database, 1337 compounds were qualitatively identified, including plant metabolites and secondary metabolites. Classify the substances at the first level and count their frequency. Based on the analytical results, the chemical constituents were categorized into 13 major classes: flavonoids, phenolic acids, organic acids, lipids, sugars, alkaloids, nucleotides and their derivatives, lignans and coumarins, terpenes, tannins, quinones, and others. In addition, the sequencing results identified a total of 1337 chemical components in the complex (the top 50 are listed in Table 2). Among them, components such as poplar extract, baicalin, colchicine, quercetin, and gallic acid have antibacterial and anti-inflammatory effects in clinical practice.

Table 2. Ingredient name and CAS number

Ingredient name	CAS
3,5,6,7,8,3',4'-Heptamethoxyflavone	1178-24-1
3,5,6,7,8,4'-Hexamethoxyflavone	34170-18-8

Nobiletin	478-01-3
5-Hydroxy-3,3',4',5',7-Pentamethoxyflavone	5084-19-5
5-Hydroxy-6,7,8,3',4'-pentamethoxyflavone	2174-59-6
Casticin	479-91-4
5,4'-Dihydroxy-3,6,7,3'-tetramethoxyflavone*	603-56-5
5,7-Dihydroxy-3,4',6,8-tetramethoxyflavone*	50461-86-4
3',4',5',5,7-Pentamethoxyflavone	53350-26-8
Tangeretin	481-53-8
Sinensetin	2306-27-6
Retusin	1245-15-4
3,7-DimethylQuercetagetin-(3',4',5,6-Tetrahydroxy-3,7-dimethoxyflavone)	59171-23-2
5,6,7,4'-Tetramethoxyflavanone	2569-77-9
5,6,3',4'-Tetrahydroxy-3,7-dimethoxyflavone	59171-23-2
5,7-Dihydroxy-3',4',5'-trimethoxyflavone	18103-42-9
5,7,8,4'-Tetramethoxyflavone	6601-66-7
Tenaxin I*	86926-52-5
Syringetin	4423-37-4
5,6,7,4'-Tetramethoxyflavone	1168-42-9
6-Hydroxy-1,2,3,7-tetramethoxyxanthone	64756-87-2
Jaceosidin	18085-97-7
5,8,4'-Trihydroxy-6,7-dimethoxyflavone	98755-25-0
Quercetin-3',4'-dimethyl ether	33429-83-3
Salvigenin	19103-54-9
6-Hydroxy-5,7,4'-trimethoxyflavone	6938-19-8
3,7-Di-O-methylquercetin	2068/2/2
Quercetin-3,3'-dimethyl ether	4382-17-6
1,3-dihydroxy-2,4,7-trimethoxyxanthen-9-one	91679-29-7
5,2'-Dihydroxy-7,8-dimethoxyflavone	41060-16-6
3-O-Methylquercetin	1486-70-0
Isorhamnetin	480-19-3
Rhamnetin	90-19-7
Gallocatechin*	3371-27-5
3'-O-Methyl-epicatechin	76549-34-3
Ganhuangemin	80366-15-0
Dihydrokaempferide	137225-59-3
Homoeriodictyol	446-71-9
Hesperetin	520-33-2
Robinetin	490-31-3
Taxifolin	480-18-2
Quercetin	117-39-5
Chrysoeriol;	491-71-4
3-Methylkaempferol	1592-70-7
Tricetin	520-31-0
4'-Hydroxy-5,7-dimethoxyflavanone	26207-67-0
Apigenin-7,4'-dimethyl ether	5128-44-9
Diosmetin*	520-34-3
Catechin*	7295-85-4
Luteoforol	24897-98-1
Eriodictyol	552-58-9
Isosakuranetin	480-43-3
3,4,2',4',6'-Pentahydroxychalcone	73692-51-0
Scutellarein	529-53-3
Aromadendrin	480-20-6

Isoscutellarein	41440-05-5
Acacetin	480-44-4
Wogonin	632-85-9
Oroxylin A	480-11-5
Datisctin	480-15-9
Kaempferol	520-18-3
Luteolin	491-70-3
Afzelechin	2545-00-8
Epiafzelechin	24808-04-6
Phloretin	60-82-2
Dihydrobaicalein	35683-17-1
Naringenin	480-41-1
Baicalein	491-67-8
Apigenin	520-36-5
Norwogonin	4443-09-8
6-Hydroxy-2'-methoxyflavone	61546-59-6
2,4,4'-trihydroxydihydrochalcone	15097-74-2
Pinocembrin	480-39-7
6,7-Dihydroxyflavone	38183-04-9
3,4'-Dihydroxyflavone	4143-64-0
Chrysin	480-40-0
D-Panthenol	81-13-0
Dihydroxyacetone phosphate	57-04-5
Rhamnose*	73-34-7
D-Fucose*	6189-71-5
D-Threonic Acid	20246-26-8
D-Threose	95-43-2
Erythrose	1758-51-6
2,3-Dihydroxypropanal	56-82-6

Enrichment of differentially expressed genes and pathways in ST cells infected with PRV:The ST cells in the Control group showed fibroblast-like, adherent growth . The ST cells in the PRV group appeared to be wrinkled, rounded, and formed clusters of grape bunch-like cells, with typical CPE phenomena such as obvious detachment and death . The half of the infection of PRV on the ST cells was $10^{-7.42}$ /0.1 mL. After PRV infection of ST cells, transcriptome sequencing identified 1650 up-regulated genes and 1359 down-regulated genes ($P < 0.01$)(Fig.1A). KEGG pathway enrichment analysis showed that these differentially expressed genes were significantly enriched in important cellular signaling pathways such as mTOR, Hippo, TGF - β , MAPK, PI3K Akt, FOXO, AMPK, and Notch. Meanwhile, significant enrichment was observed in pathological and physiological processes related to neurodegenerative disease pathways, cellular aging, viral carcinogenesis, leukocyte transendothelial migration, and Fc γ R-mediated phagocytosis(Fig.1B). In the testes, the FOXO signaling pathway is crucial for maintaining male reproductive health by regulating apoptosis of germ cells, oxidative stress response, and supporting cell function. Therefore, the FOXO signaling pathway was selected for subsequent experiments.

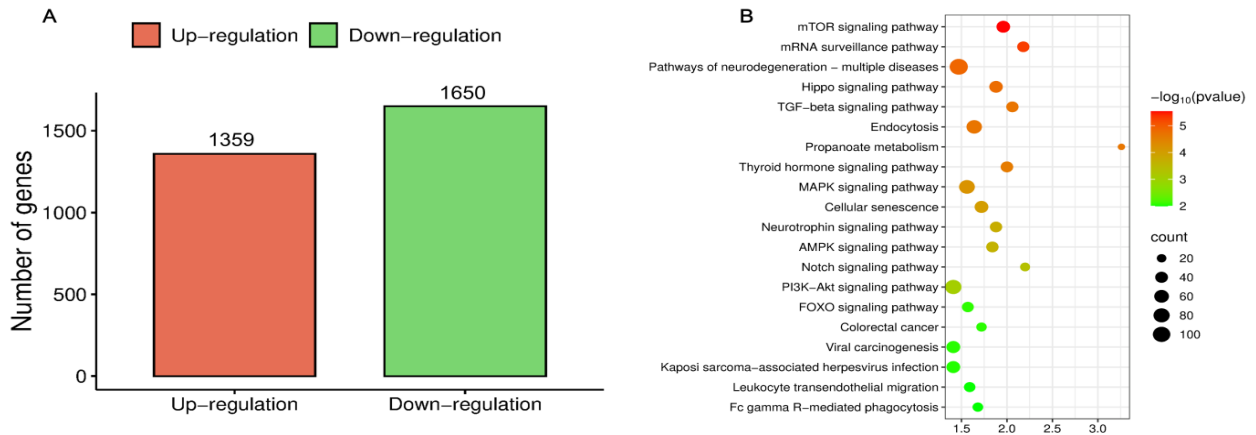


Fig.1 Transcriptome sequencing results of PRV infected ST cells

(A) Genes with significant differences. **(B)** KEGG pathway enrichment analysis.

The effect of inhibiting FOXO signaling pathway on PRV infected ST cells: The proliferation rates of ST cells were all higher than 70% at inhibitor AS1842856 concentrations $\leq 100 \mu\text{M}$ (Fig. 2A). Based on these results, 25 μM was selected as the subsequent experimental concentration. After treatment with the AS1842856 inhibitor, the viral copy numbers of the AS1842856 +PRV group were all extremely significantly reduced. Compared with the Control group, the virus copy number of the PRV group was significantly increased ($P < 0.01$), and the virus copy number of the PRV group was the highest. Notably, the AS1842856+PRV group showed a significant reduction in viral load compared to the PRV group ($P < 0.01$) (Fig. 2B). Correspondingly, PRV infection up-regulated FOXO1 and FOXO4 mRNA expression while down-regulating FOXO3 compared to the blank group. Conversely, FOXO pathway inhibition with AS1842856 reversed this pattern, leading to down-regulation of FOXO1 and FOXO4, and up-regulation of FOXO3 (Fig. 2C-E).

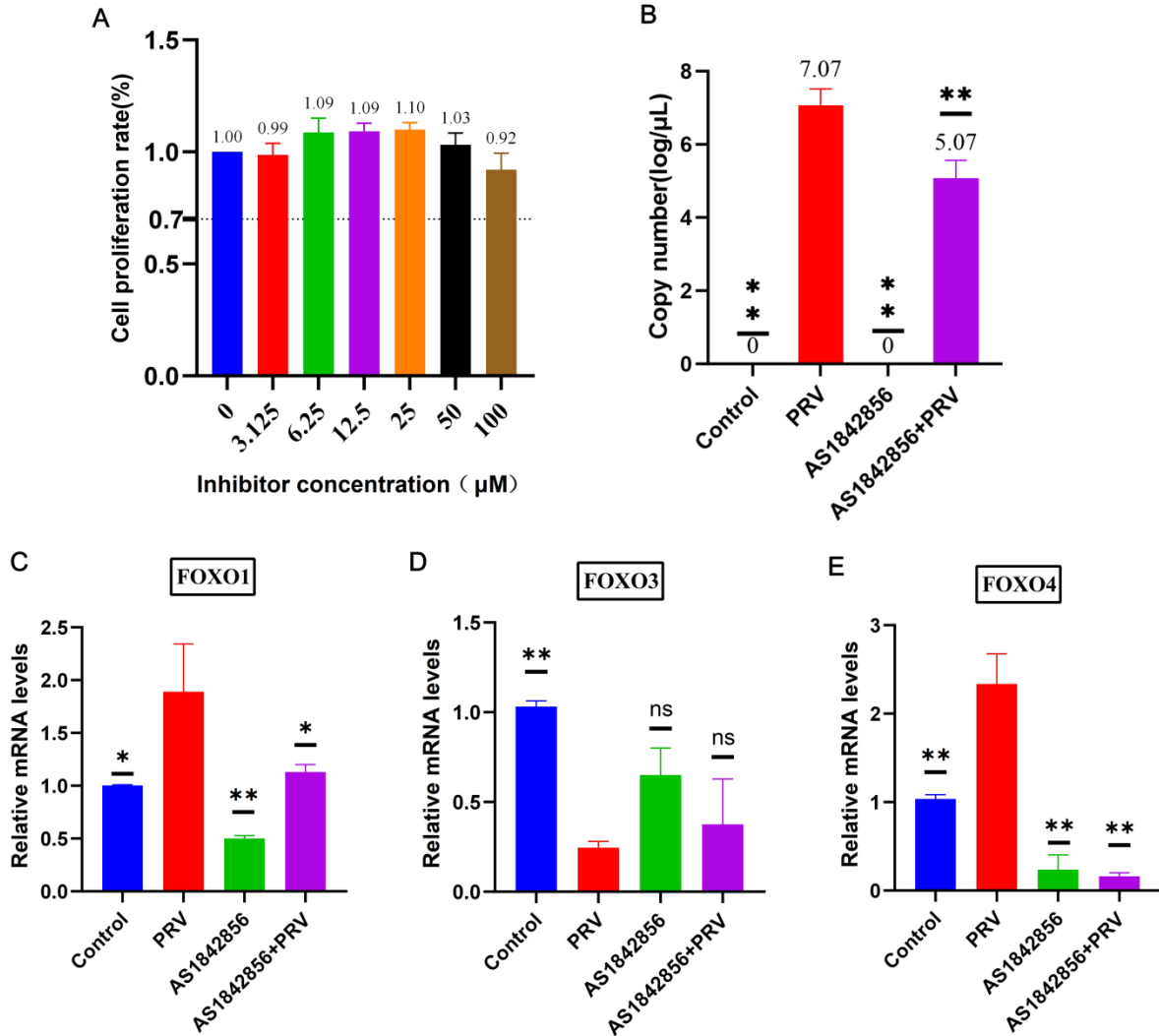


Fig.2 The effect of inhibiting FOXO signaling pathway on PRV infected ST cells (A)Effect of inhibitors on ST cell viability in blocking mode. (B) Effect of inhibitors on PRV copy number. (C) Effect of inhibitor on FOXO1. (D) Effect of inhibitor on FOXO3. (E) Effect of inhibitor on FOXO4.

Effects of RS on FOXO signaling pathway in ST cells:The proliferation rate of the ST cells was higher than 70% at the concentration of RS ≤ 125 $\mu\text{g}/\text{mL}$ in all of them. This concentration was determined to be nontoxic to ST cells (Fig. 3A). Therefore, 50 $\mu\text{g}/\text{mL}$, 25 $\mu\text{g}/\text{mL}$, and 12.5 $\mu\text{g}/\text{mL}$ were selected as the conditions for further investigation of the in vitro anti-PRV study of RS. Compared with the blank group, the virus copy number of the PRV group was significantly increased ($P < 0.01$), and the virus copy number of the PRV group was the highest. All RS-treated groups exhibited a significant reduction in viral copy number compared to the PRV-infected group ($P < 0.01$), demonstrating a clear dose-dependent inhibitory effect (Fig. 3B). At the transcriptional level, PRV infection markedly up-regulated FOXO1 and FOXO4 mRNA expression while down-regulating FOXO3 compared to the Control group. This infection-induced expression pattern was effectively reversed by RS treatment, with all three dosage groups (RS-H, RS-M, and RS-L) showing significant down-regulation of FOXO1 and FOXO4 accompanied by up-regulation of FOXO3 (Fig. 3C-E).

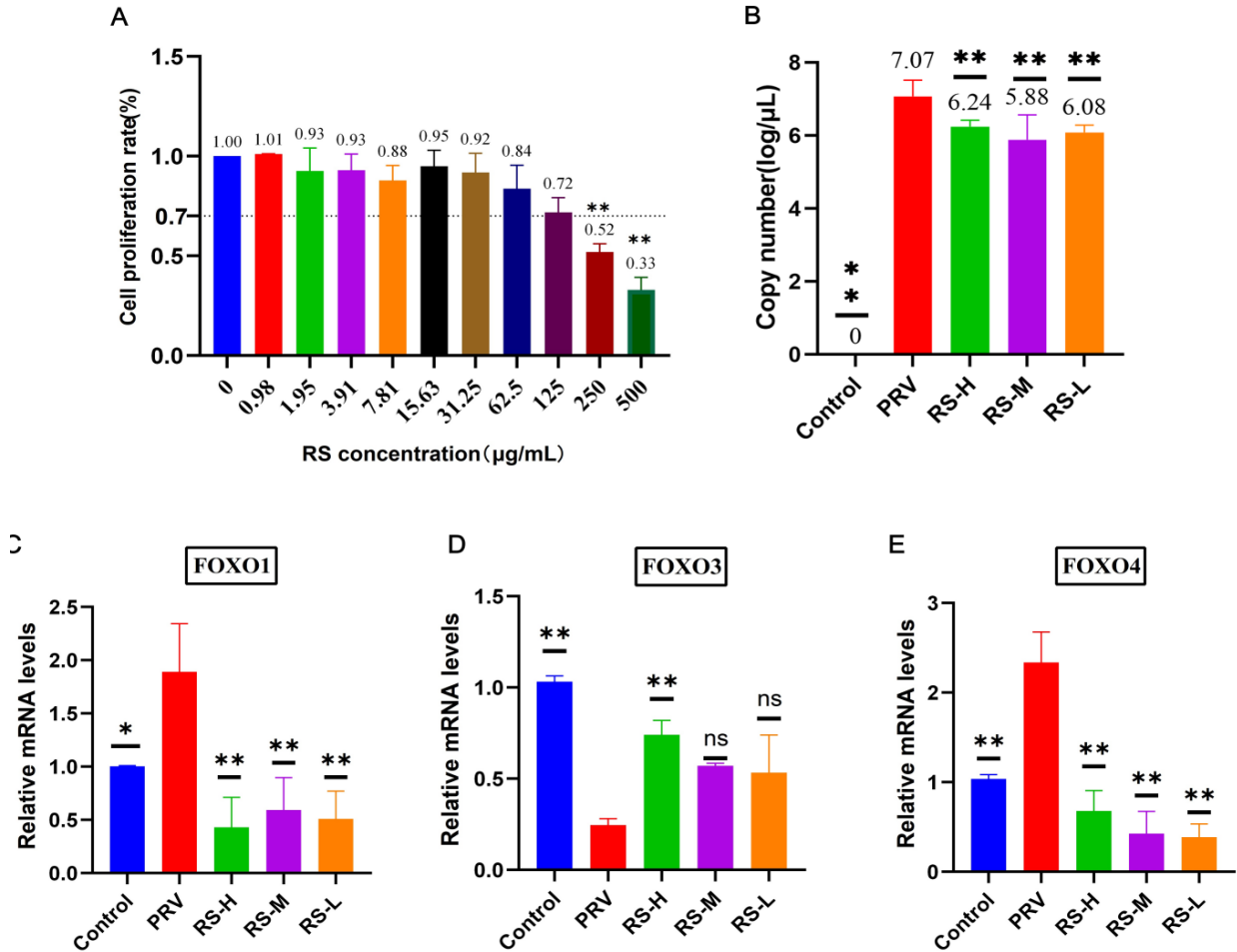


Fig.3 Effects of RS on FOXO signaling pathway in ST cells

(A) Effect of RS on ST cell viability in blocking mode. (B) Effect of RS on PRV copy number. (C) Effect of RS on FOXO1 in ST cells. (D) Effect of RS on FOXO3 in ST cells. (E) Effect of RS on FOXO4 in ST cells.

Effects of PRV infection induced testicular damage in mice: Inflammatory symptoms were observed after PRV infection (Fig.4A), but there was no significant change in testicular index (Fig.4D). Compared with the blank group, in the PRV group, the seminiferous tubules disappeared, spermatogonia, spermatocytes, and spermatocytes were broken, the spermatogenic epithelium was severely disrupted, with the appearance of loose spermatogenic epithelium and large vacuolated structures, the spermatogenic tubules disappeared, and fewer spermatozoa or disappeared were observed. Compared with the PRV group, in the group with RS, normal seminiferous tubules and spermatozoa within them were observed, large vacuolated structures of the seminiferous epithelium were ameliorated, and spermatogenic cells, spermatogonia, and spermatocytes were normal (Fig.4B). Measurement of testicular PRV concentration showed the highest viral load in the PRV group, which was significantly higher than the Control group. All RS-treated groups exhibited a dose-dependent reduction in testicular viral load compared to the PRV-infected group (Fig. 4C). Concurrently, while PRV infection significantly reduced sperm counts ($P < 0.05$), administration of RS at various doses led to a marked recovery in sperm numbers (Fig. 4E).

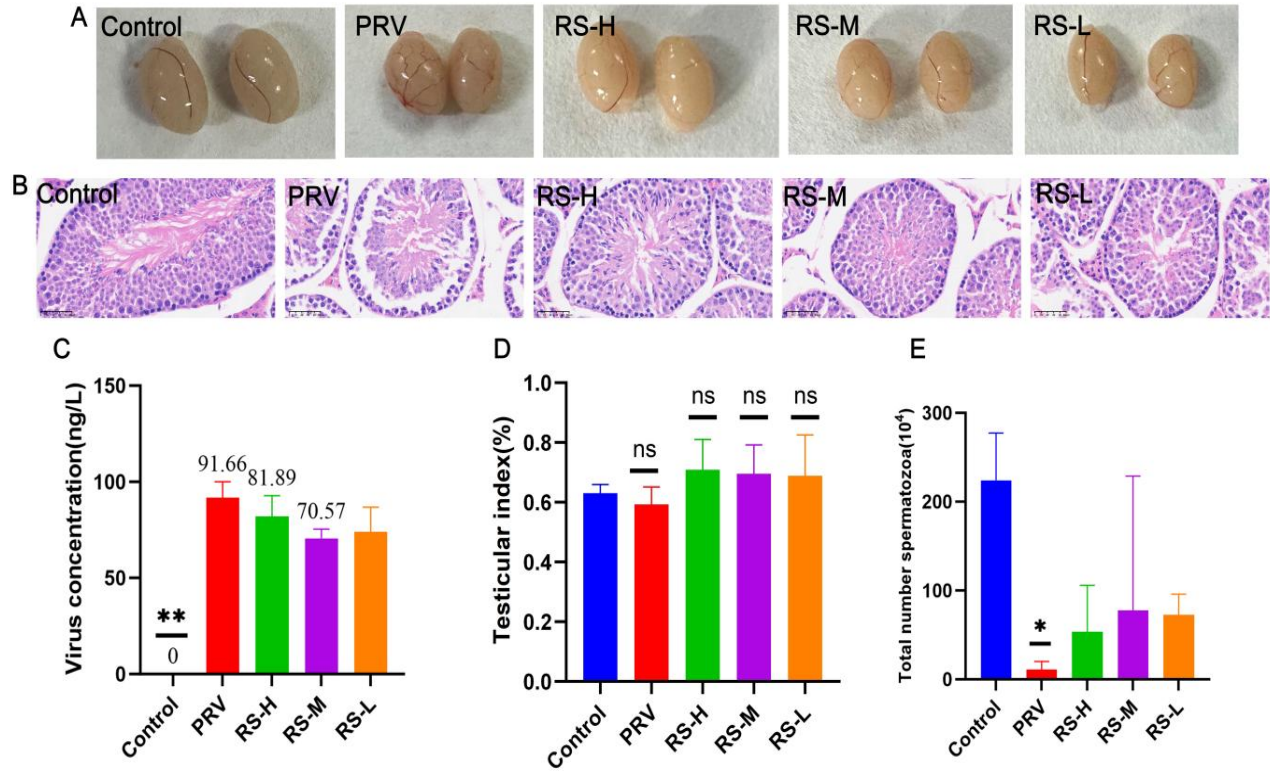


Fig.4 The effects of PRV and different doses of RS on testes (A)Photos of testicular tissue. (B) HE sections 400×. (C) Virus concentration. (D) Testicular index . (E) Sperm counts.

Effect on FOXO signaling pathway in PRV-infected mice:PRV infection differentially regulates FOXO family members at the transcriptional level: FOXO1 and FOXO4 expression is upregulated, while FOXO3 expression is downregulated. These infection-induced expression patterns were effectively reversed by RS treatment, with all three doses consistently down-regulating FOXO1/FOXO4 and promoting FOXO3 restoration (Fig. 5A-C).

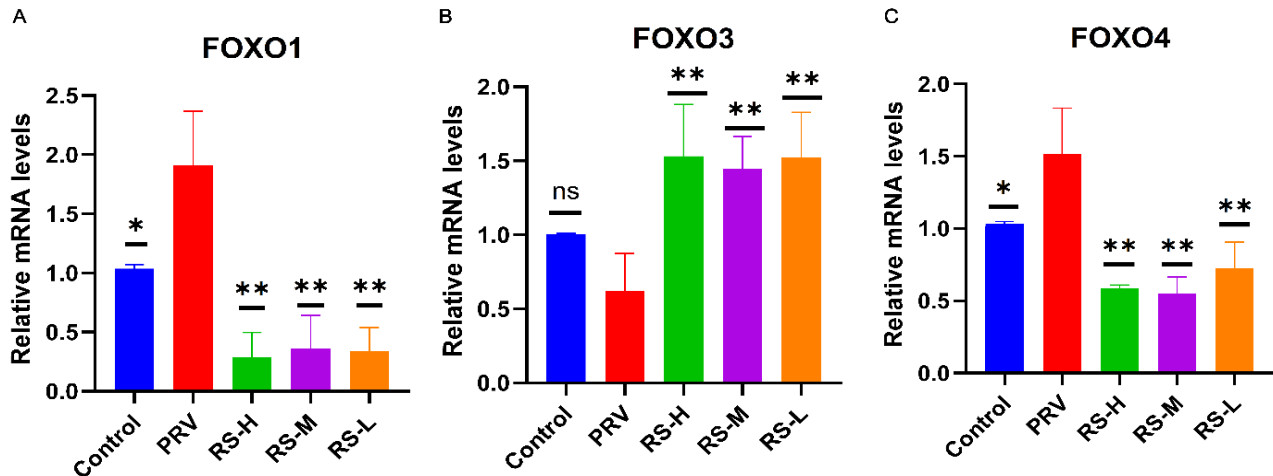


Fig.5 FOXO1, FOXO3, FOXO4 mRNA expression in the testes (A) Effect of RS on FOXO1 in the testes. (B) Effect of RS on FOXO3 in the testes. (C) Effect of RS on FOXO4 in the testes.

DISCUSSION

Pseudorabies virus (PRV) infection can cause severe reproductive system diseases, but its specific molecular mechanisms remain incompletely understood. Our transcriptomic analysis initially identified several enriched pathways, including mTOR, MAPK, and PI3K-Akt. However, we focused on the FOXO pathway because of its pivotal and specific functions in the male reproductive system. FOXO transcription factors are master regulators of cellular homeostasis, and within the testes, they are crucial for the maintenance of spermatogonial stem cells and the support of spermatogenesis (Goertz *et al.*, 2011). Transcriptome sequencing analysis in this study revealed that PRV infection of ST cells significantly activates the FOXO signaling pathway, suggesting its crucial role in the infection process. Further studies confirmed that inhibiting the FOXO pathway markedly reduces viral replication within ST cells. PRV infection differentially regulates FOXO family members: FOXO1 and FOXO4 expression is upregulated, while FOXO3 expression is downregulated. The compound RS exhibits potent anti-PRV activity in both cellular and animal models by reversing PRV-induced FOXO expression imbalance—specifically, suppressing FOXO1 and FOXO4 while activating FOXO3 at the transcriptional level.

Previous studies indicate that FOXO transcription factors perform critical functions in the male reproductive system. FOXO1 is highly expressed in undifferentiated spermatogonia, and its sustained expression can lead to testicular atrophy and reduced sperm count, disrupting male reproductive homeostasis (Goertz *et al.*, 2011). FOXO4 participates in regulating testicular interstitial cell apoptosis and influences testosterone levels during aging (Shi *et al.*, 2023). Consistent with these findings, our study demonstrates that PRV infection induces elevated FOXO1 and FOXO4 expression, potentially exacerbating testicular cell apoptosis and dysfunction, while FOXO3 downregulation may diminish its anti-apoptotic or antioxidant protective effects. RS intervention reverses this abnormal expression pattern, suggesting it may protect testicular tissue from PRV-induced damage by rebalancing the FOXO pathway.

Beyond the FOXO pathway, RS contains multiple bioactive components, including gallic acid, baicalin, and quercetin. These compounds may exert antiviral effects through multiple targets and pathways. For instance, baicalin regulates apoptosis via the NF- κ B pathway (Shen *et al.*, 2019), epigallocatechin gallate inhibits PRV replication through the JAK/STAT pathway (Song *et al.*, 2025), in addition to its antioxidant effects, quercetin also exhibits notable anti-inflammatory capabilities (Azeem *et al.*, 2023; Shorobi *et al.*, 2023; Wang *et al.*, 2022). The synergistic interaction of these components likely enhances RS's antagonistic effect against PRV infection.

In animal models, PRV infection induced pathological damage in mouse testicular tissue, including vacuolation of the spermatogenic epithelium, disorganized arrangement of spermatogenic cells, and a significant reduction in sperm count, consistent with previously reported PRV reproductive toxicity manifestations (Lin *et al.*, 2012; Sehl *et al.*, 2020; Su *et al.*, 2016). RS intervention not only significantly reduced viral load in testicular tissue but also improved seminiferous tubule structural integrity and partially restored sperm count, further confirming its potential in mitigating PRV reproductive toxicity.

Currently, flavonoid and polysaccharide compounds are receiving widespread attention as potential anti-PRV therapeutics. For instance, myricetin inhibits PRV replication and alleviates inflammatory responses by regulating MAPK and NF- κ B pathways (Hu *et al.*, 2022), while platycodin polysaccharides antagonize PRV by suppressing autophagy via the Akt/mTOR pathway (Lv *et al.*, 2020; Wang *et al.*, 2024). The RS complex in this study, containing both flavonoid and polysaccharide components, exhibits similar broad-spectrum antiviral potential, providing a theoretical basis for its further development as an anti-PRV drug.

Conclusion: Transcriptomic analysis and cell experiments confirmed that targeting the FOXO signaling pathway significantly inhibits PRV replication in ST cells. PRV differentially regulates FOXO family members, upregulating FOXO1/FOXO4 and downregulating FOXO3. Compound RS reverses this imbalance at the transcriptional level—suppressing FOXO1/FOXO4 while restoring FOXO3 expression—thereby exerting potent anti-PRV effects in both cellular and animal models. In vivo, RS treatment reduced testicular viral load, improved seminiferous tubule integrity, and increased sperm count, offering a promising intervention for PRV-induced reproductive toxicity.

REFERENCES

- An, T. Q., J. M. Peng, Z. J. Tian, H. Y. Zhao, N. Li, Y. M. Liu, J. Z. Chen, C. L. Leng, Y. Sun, D. Chang and G. Z. Tong (2013). Pseudorabies virus variant in Bartha-K61-vaccinated pigs, China, 2012. *Emerg Infect Dis.* 19(11): 1749-1755. <http://doi.org/10.3201/eid1911.130177>
- Azeem, M., M. Hanif, K. Mahmood, N. Ameer, F. Chughtai and U. Abid (2023). An insight into anticancer, antioxidant, antimicrobial, antidiabetic and anti-inflammatory effects of quercetin: a review. *Polym Bull (Berl).* 80(1): 241-262. <http://doi.org/10.1007/s00289-022-04091-8>

- Goertz, M. J., Z. Wu, T. D. Gallardo, F. K. Hamra and D. H. Castrillon (2011). Foxo1 is required in mouse spermatogonial stem cells for their maintenance and the initiation of spermatogenesis. *J Clin Invest.* 121(9): 3456-3466. <http://doi.org/10.1172/JCI157984>
- Hu, H., Z. Hu, Y. Zhang, H. Wan, Z. Yin, L. Li, X. Liang, X. Zhao, L. Yin, G. Ye, Y. F. Zou, H. Tang, R. Jia, Y. Chen, H. Zhou and X. Song (2022). Myricetin inhibits pseudorabies virus infection through direct inactivation and activating host antiviral defense. *Front Microbiol.* 13(2022): 985108. <http://doi.org/10.3389/fmicb.2022.985108>
- Jacobs, F. M., L. P. van der Heide, P. J. Wijchers, J. P. Burbach, M. F. Hoekman and M. P. Smidt (2003). FoxO6, a novel member of the FoxO class of transcription factors with distinct shuttling dynamics. *J Biol Chem.* 278(38): 35959-35967. <http://doi.org/10.1074/jbc.M302804200>
- Lin, Y., D. Wu, W. X. Zeng, Z. F. Fang and L. Q. Che (2012). Effect of threonine on immunity and reproductive performance of male mice infected with pseudorabies virus. *Animal.* 6(11): 1821-1829. <http://doi.org/10.1017/S1751731112000833>
- Lv, L., M. Cao, J. Bai, L. Jin, X. Wang, Y. Gao, X. Liu and P. Jiang (2020). PRV-encoded UL13 protein kinase acts as an antagonist of innate immunity by targeting IRF3-signaling pathways. *Vet Microbiol.* 250(2020): 108860. <http://doi.org/10.1016/j.vetmic.2020.108860>
- Pan, Q., Y. Wang, C. Song, S. Pu and X. Shu (2022). Safety Evaluation of The Compound of *Rodgersia sambucifolia* Hemsl. Flavonoids and *Scutellaria baicalensis* Georgi Polysaccharide. *Feed Industry.* 43(23): 33-37. <http://doi.org/10.13302/j.cnki.fi.2022.23.007>
- Sehl, J. and J. P. Teifke (2020). Comparative Pathology of Pseudorabies in Different Naturally and Experimentally Infected Species-A Review. *Pathogens.* 9(8): 633. <http://doi.org/10.3390/pathogens9080633>
- Shen, J., J. Cheng, S. Zhu, J. Zhao, Q. Ye, Y. Xu, H. Dong and X. Zheng (2019). Regulating effect of baicalin on IKK/IKB/NF- κ B signaling pathway and apoptosis-related proteins in rats with ulcerative colitis. *Int Immunopharmacol.* 73(2019): 193-200. <http://doi.org/10.1016/j.intimp.2019.04.052>
- Shi, L., A. Zhang, H. Liu and H. Wang (2023). Deletion of the foxO4 Gene Increases Hypoxia Tolerance in Zebrafish. *Int J Mol Sci.* 24(10): 8942. <http://doi.org/10.3390/ijms24108942>
- Shorobi, F. M., F. Y. Nisa, S. Saha, M. Chowdhury, M. Srisuphanunt, K. H. Hossain and M. A. Rahman (2023). Quercetin: A Functional Food-Flavonoid Incredibly Attenuates Emerging and Re-Emerging Viral Infections through Immunomodulatory Actions. *Molecules.* 28(3): 938. <http://doi.org/10.3390/molecules28030938>
- Shu, X., Y. Zhang, X. Zhang, Y. Zhang, Y. Shu, Y. Wang, Z. Zhang and C. Song (2024). Therapeutic and immune-regulation effects of *Scutellaria baicalensis* Georgi polysaccharide on pseudorabies in piglets. *Front Vet Sci.* 11(2024): 1356819. <http://doi.org/10.3389/fvets.2024.1356819>
- Song, Y., X. Zhao, Y. Chen, X. Yu, T. Su, J. Wang, T. He, Z. Yin, R. Jia, X. Zhao, X. Zhou, L. Li, Y. Zou, M. Li, D. Zhang, Y. Zhang and X. Song (2025). The antiviral activity of myricetin against pseudorabies virus through regulation of the type I interferon signaling pathway. *J Virol.* 99(1): e156724. <http://doi.org/10.1128/jvi.01567-24>
- Su, D., S. Wu, J. Guo, X. Wu, Q. Yang and X. Xiong (2016). Protective effect of resveratrol against pseudorabies virus-induced reproductive failure in a mouse model. *Food Sci Biotechnol.* 25(1): 103-106. <http://doi.org/10.1007/s10068-016-0105-8>
- Tran, T. Q. and C. Kioussi (2021). Pitx genes in development and disease. *Cell Mol Life Sci.* 78(11): 4921-4938. <http://doi.org/10.1007/s00018-021-03833-7>
- Wang, C., L. Li, X. Zhai, H. Chang and H. Liu (2024). Evasion of the Antiviral Innate Immunity by PRV. *Int. J. Mol. Sci.* 25(23). <http://doi.org/10.3390/ijms252313140>
- Wang, G., Y. Wang, L. Yao, W. Gu, S. Zhao, Z. Shen, Z. Lin, W. Liu and T. Yan (2022). Pharmacological Activity of Quercetin: An Updated Review. *Evid Based Complement Alternat Med.* 2022(1): 3997190. <http://doi.org/10.1155/2022/3997190>
- Zhao, T., H. Tang, L. Xie, Y. Zheng, Z. Ma, Q. Sun and X. Li (2019). *Scutellaria baicalensis* Georgi. (Lamiaceae): a review of its traditional uses, botany, phytochemistry, pharmacology and toxicology. *J Pharm Pharmacol.* 71(9): 1353-1369. <http://doi.org/10.1111/jphp.13129>
- Zheng, H. H., P. F. Fu, H. Y. Chen and Z. Y. Wang (2022). Pseudorabies Virus: From Pathogenesis to Prevention Strategies. *Viruses.* 14(8): 1638. <http://doi.org/10.3390/v14081638>
- Zhou, L., X. Su, B. Li, C. Chu, H. Sun, N. Zhang, B. Han, C. Li, B. Zou, Y. Niu and R. Zhang (2019). PM2.5 exposure impairs sperm quality through testicular damage dependent on NALP3 inflammasome and miR-183 / 96 / 182 cluster targeting FOXO1 in mouse. *Ecotoxicol. environ. saf.* 169(2019): 551-563. <http://doi.org/10.1016/j.ecoenv.2018.10.108>